



# Equidistant precipitate pattern formation behind a propagating chemical front

István Lagzi<sup>\*</sup>, Dániel Kármán

*Department of Physical Chemistry, Eötvös University, Pázmány P. Sétány 1.A, P.O. Box 32, Budapest H-1518, Hungary*

Received 7 January 2003; in final form 25 February 2003

## Abstract

Formation of one- and two-dimensional equidistant precipitate patterns due to the coupling of an autocatalytic chemical front with a precipitation reaction was studied numerically. A simple six-variable model based on a cubic autocatalytic reaction has been defined and investigated, where the precipitation step contained a diffusive intermediary species. Simulations show that such a hypothetical reaction–diffusion system can lead to formation of equidistantly striped or more complex patterns.

© 2003 Elsevier Science B.V. All rights reserved.

## 1. Introduction

Liesegang patterning is an example of periodic pattern formation in reaction–diffusion systems [1]. These patterns are produced by a precipitation reaction behind a moving reaction front. In classical Liesegang systems position of the last band is proportional to the square root of time elapsed until its formation:

$$X_n \propto t_n^{1/2},$$

where  $X_n$  is the distance of the  $n$ th precipitate zone measured from the junction point of the two electrolytes while  $t_n$  is the time elapsed until appearance of the  $n$ th band [2]. This relation is the time law. Liesegang patterns usually obey another empirical scaling law, the so-called spacing law. According to

this for large enough  $n$  positions of precipitate zones are members of a geometrical series, that is

$$X_{n+1}/X_n = 1 + p, \quad \text{if } n \rightarrow \infty,$$

where  $(1 + p)$  is the spacing coefficient [3], value of which usually falls to the range  $0.05 \leq p \leq 0.4$ . Width of the zones follows a similar scaling. Width of the  $n$ th band ( $w_n$ ) is an increasing function of  $n$  according to the following simple relation:

$$w_n \propto X_n^\alpha,$$

where  $\alpha > 0$  [4–7].

The first propagating chemical fronts were observed by Luther in the early 1900s [8]. He has shown that these fronts travel with constant velocity, which depends on a pseudo-first-order rate constant and the diffusion coefficient of the autocatalyst. Recently, various chemical fronts and pattern formation due to diffusion driven instability in such systems were extensively studied [9–13].

<sup>\*</sup> Corresponding author. Fax: +3612090602.

E-mail address: [lagzi@vuk.chem.elte.hu](mailto:lagzi@vuk.chem.elte.hu) (I. Lagzi).

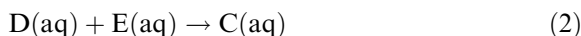
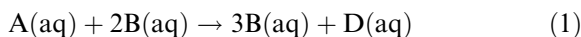
In 1952 Turing [14] reported that the homogeneous state of chemical species may lose its stability if diffusion coefficients of species are different. As a result classical Turing patterns emerge, which consist of stationary equidistant spots and stripes [15–17]. These structures are supposed to appear in various biological systems.

The second technique to produce equidistant patterns is the flow-distributed oscillations [18–20]. Kuznetsov et al. and Andresen et al. [21,22] investigated in these systems the condition for pattern formation using the Brusselator model, while Kaern and Menzinger [23] have demonstrated existence of such equidistant structures experimentally.

In the present work we propose a new mechanism based on the coupling of a simple autocatalytic front with a precipitation process, as an alternative to Liesegang, Turing and FDO patterns.

## 2. Mathematical formulation of the model

Chemical equations describing a simple cubic autocatalytic reaction and a precipitation step coupled with it are the following:



Here A(aq) is the reactant, B(aq) is the autocatalyst, D(aq) is the product of the autocatalytic reaction, which reacts with E(aq) and forms the intermediate species C(aq). This latter will transform into precipitate P(s) above a critical concentration. The system is normally highly supersaturated therefore reaction (3) is practically irreversible.

Dynamics of the system above can be described by the following reaction–diffusion differential equations:

$$\frac{\partial \alpha}{\partial \tau} = D_\alpha \nabla^2 \alpha - k_1 \alpha \beta^2, \quad (4)$$

$$\frac{\partial \beta}{\partial \tau} = D_\beta \nabla^2 \beta + k_1 \alpha \beta^2, \quad (5)$$

$$\frac{\partial \gamma}{\partial \tau} = D_\gamma \nabla^2 \gamma + k_2 \delta \varepsilon - \Psi(\kappa_2, \gamma, \gamma^*) - \kappa_3 \gamma \pi, \quad (6)$$

$$\frac{\partial \delta}{\partial \tau} = D_\delta \nabla^2 \delta + k_1 \alpha \beta^2 - k_2 \delta \varepsilon, \quad (7)$$

$$\frac{\partial \varepsilon}{\partial \tau} = D_\varepsilon \nabla^2 \varepsilon - k_2 \delta \varepsilon, \quad (8)$$

$$\frac{\partial \pi}{\partial \tau} = \Psi(\kappa_2, \gamma, \gamma^*) + \kappa_3 \gamma \pi, \quad (9)$$

where  $\alpha$ ,  $\beta$ ,  $\gamma$ ,  $\delta$  and  $\varepsilon$  are the dimensionless concentrations of A(aq), B(aq), C(aq), D(aq) and E(aq), respectively,  $\pi$  is the dimensionless amount of precipitate P(s).  $D_\alpha$ ,  $D_\beta$ ,  $D_\gamma$ ,  $D_\delta$  and  $D_\varepsilon$  are the dimensionless diffusion coefficients of the corresponding species.  $k_1$ ,  $k_2$ ,  $\kappa_2$  and  $\kappa_3$  are dimensionless rate coefficients of reactions (1)–(3), respectively and  $\tau$  is the dimensionless time. The two terms in (9) correspond to homogenous nucleation ( $\Psi(\kappa_2, \gamma, \gamma^*)$ ) that is followed by autocatalytical crystal growth ( $\kappa_3 \gamma \pi$ ). The definition of the function  $\Psi(\kappa_2, \gamma, \gamma^*)$  in a 1D simulation is the following:

$$\Psi(\kappa_2, \gamma, \gamma^*) = \kappa_2 \Theta(\gamma(x, \tau) - \gamma^*) \gamma \quad (10)$$

while in 2D

$$\Psi(\kappa_2, \gamma, \gamma^*) = \kappa_2 \Theta(\gamma(x, y, \tau) - \gamma^*) \Theta(Pr - r(x, y, \tau)) \gamma. \quad (11)$$

Here  $Pr$  is the user-defined probability,  $r(x, y, \tau)$  is a random number between 0 and 1, which is individually generated for every grid point in every time step while  $\Theta$  is the Heaviside step function.  $\kappa_2 \Theta(\gamma - \gamma^*) \gamma$  is the supersaturation term and  $\Theta(Pr - r)$  is the probabilistic (fluctuating) term.  $\kappa_2$  is the rate coefficient of the homogenous nucleation process. Stochastic noise can be switched off if  $Pr$  is chosen to be unity.

Eqs. (4) and (5) describe the evolution of a simple cubic autocatalytic reaction front. The subset of our model, which describes formation of the precipitate, contains a diffusive intermediate species between the reacting electrolytes and the final product [7]. Such intermediate species approaches are often used for description of Liesegang patterns [7,24]. When the local concentration of the intermediar reaches some threshold value ( $\gamma^*$ ) precipitation takes place. Parallel with this

concentration  $\gamma$  goes to zero wherever some precipitate already exists.

Eqs. (4)–(9) were solved numerically using an explicit Euler method with Neumann boundary conditions. The Laplace operator was discretised in 2D using a nine-point approximation. In all of the simulations the following parameter set was used:  $D_\alpha = D_\beta = D_\gamma = D_\delta = D_\epsilon = 0.8$ ,  $k_1 = k_2 = 2.5 \times 10^{-1}$ ,  $\kappa_2 = \kappa_3 = 4.9$ . Value of  $\gamma^*$  was varied between 0.12 and 0.40, while the initial conditions were the following:

$$\alpha(\tau = 0, x, y) = \alpha_0 \Theta(10 - x)$$

$$\beta(\tau = 0, x, y) = \beta_0 \Theta(x - 10)$$

$$\epsilon(\tau = 0, x, y) = \epsilon_0 \Theta(10 - x)$$

$$\pi(\tau = 0, x, y) = \gamma(\tau = 0, x, y) = \delta(\tau = 0, x, y) = 0,$$

( $\alpha_0 = \beta_0 = \epsilon_0 = 1.0$ ). Grid spacing was  $\Delta h = 0.4$  while length of a time step was  $\Delta \tau = 10^{-3}$ .

### 3. Results and discussion

Fig. 1 shows the evolution diagram of the one-dimensional pattern obtained. In case of normal Liesegang patterning positions of precipitate zones

are members of a geometrical series while movement of the reaction front producing them follows a purely diffusive kinetics [1–7]. Width of zones increases with their distance measured from the junction point of the electrolytes. Although our system contains a similar reaction front that produces an immobile reaction product our observations are markedly different compared to these patterning trends. In our case formation of the bands follows a linear scaling in time while their arrangement is equidistant in space. Thickness of the bands also becomes constant after a transient period. Causes of these differences lie in the different dynamics of the systems. In case of Liesegang patterning the outer electrolyte can move only by diffusion. Distance of the reaction–diffusion front measured from the junction point of the two electrolytes is proportional to the square root of time. The time law is a direct consequence of this dynamics.

In our case formation of bands is provoked by the propagation of an autocatalytic chemical front, which moves by constant velocity. This maintains a constant concentration of the outer electrolyte (D(aq)) behind the front and from dynamical point of view roughly corresponds to a Liesegang experiment performed in an electric field

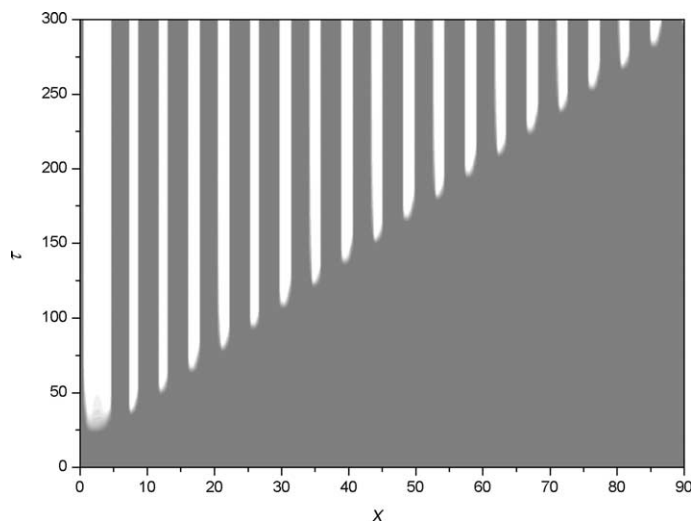


Fig. 1. Evolution of a one-dimensional pattern ( $\gamma^* = 0.2$ ). Precipitate zones are represented by white stripes. The first wider zone corresponds to a transient state of the system. After this thickness and spacing of zones becomes constant which means that evolution of such a pattern follows a linear scaling both in space and time.

[25]. In the latter case increase of the strength of the electric field makes the velocity of migration constant and causes equidistant patterning. As we were most interested in the distribution of the final reaction product we mainly examined the parameters, which are directly influencing it. The detailed numerical study has shown that patterning trends

are highly influenced by the threshold value  $\gamma^*$ . Fig. 2 illustrates this dependence for some different values of it. As can be seen width of the zones decreases while wavelength of the pattern increases with increasing values of  $\gamma^*$ .

Fig. 3 shows results of a 2D stochastic simulation in which formation of the precipitate from

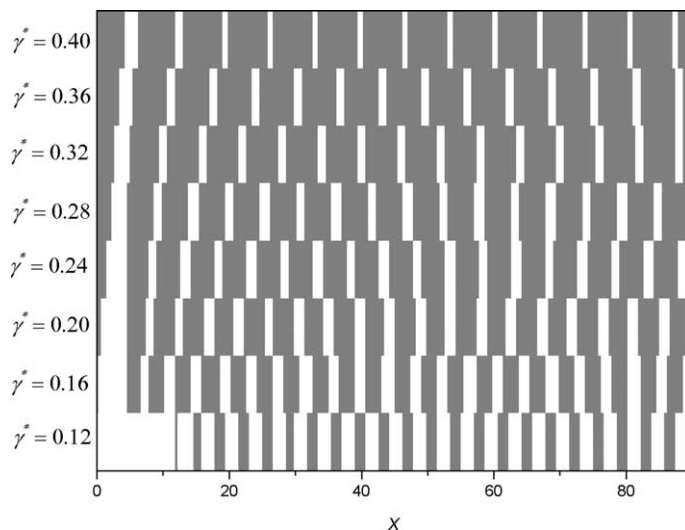


Fig. 2. Change of the spatial distribution of the precipitate in various 1D simulations. Value of  $\gamma^*$  was varied at  $\tau = 300$ .

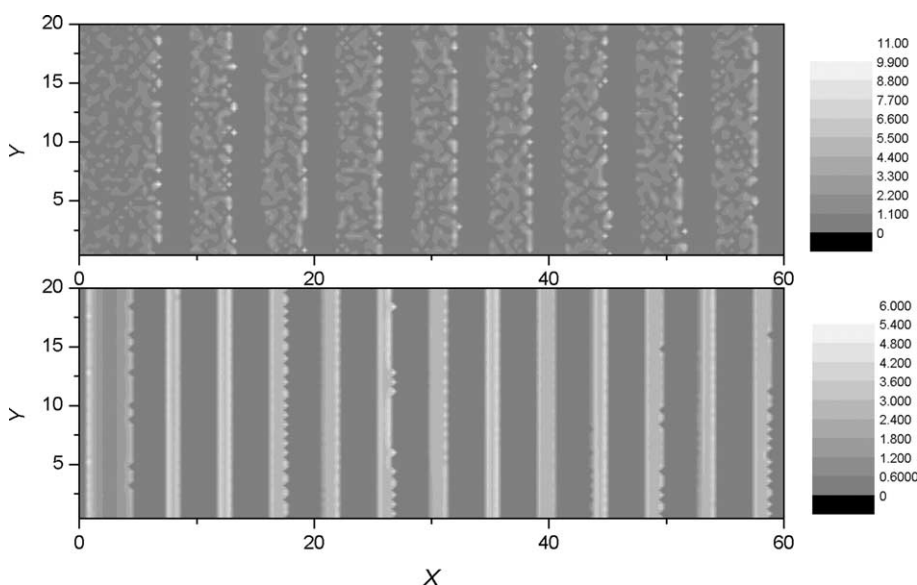


Fig. 3. Two-dimensional stochastic patterns at  $\tau = 300$  developed from planar initiation. Values of the input parameters:  $\gamma^* = 0.2$ ,  $Pr = 0.0005$  (top) and  $Pr = 0.5$  (bottom). The front has travelled from left to right.

C(aq) was a probabilistic process. Büki et al. [26] applied a similar probabilistic approach in order to generate two-dimensional stochastic Liesegang patterns. Practically it means that in every point where concentration of C(aq) reached the critical value ( $\gamma^*$ ) precipitation could take place only by a certain probability ( $Pr$ ). This causes a more complex patterning dynamics. Distribution of matter inside the zones becomes non-uniform, which is due to the stochastic noise applied.

We have proposed a model for the formation of equidistant and more complex precipitate patterns. It has been shown by numerical simulations that coupling of the reaction front of a cubic autocatalytic reaction with a precipitation process can lead to formation of such chemical patterns. The precipitation mechanism contained a diffusive intermediate species.

### Acknowledgements

The authors would like thank Drs. A. Büki, T. Turányi, Á. Tóth and D. Horváth for the helpful discussions.

### References

- [1] R.E. Liesegang, Naturwiss. Wochenschr. 11 (1896) 353.
- [2] H.W. Morse, G.W. Pierce, Proc. Am. Acad. Arts Sci. 38 (1903) 625.
- [3] K. Jablczynski, Bull. Soc. Chim. Fr. 33 (1923) 1592.
- [4] K.M. Pillai, V.K. Vaidyan, M.A. Ittyachan, Colloid Polym. Sci. 258 (1980) 831.
- [5] S.C. Müller, S. Kai, J. Ross, J. Phys. Chem. 86 (1982) 4078.
- [6] B. Chopard, P. Luthi, M. Droz, Phys. Rev. Lett. 72 (1994) 1384.
- [7] M. Droz, J. Magnin, M. Zrinyi, J. Chem. Phys. 110 (1999) 9618.
- [8] R. Luther, Z. Elektrochem. 12 (1906) 596.
- [9] L. Szivoczka, I. Nagypál, E. Boga, J. Am. Chem. Soc. 111 (1989) 2842.
- [10] D. Horváth, V. Petrov, S.K. Scott, K. Showalter, J. Chem. Phys. 98 (1993) 6332.
- [11] D. Horváth, K. Showalter, J. Chem. Phys. 102 (1995) 2471.
- [12] Á. Tóth, I. Lagzi, D. Horváth, J. Phys. Chem. 100 (1996) 14837.
- [13] D. Horváth, Á. Tóth, J. Chem. Phys. 108 (1998) 1447.
- [14] A.M. Turing, Phil. Trans. R. Soc. London B 237 (1952) 37.
- [15] V. Casters, E. Dulos, J. Boissonade, P. De Kepper, Phys. Rev. Lett. 64 (1990) 2953.
- [16] Q. Ouyang, H.L. Swinney, Nature 352 (1991) 610.
- [17] I.R. Epstein, I. Lengyel, S. Kádár, M. Kagan, M. Yokoyama, Phys. A 188 (1992) 26.
- [18] J.R. Bamforth, S. Kalliadasis, J.H. Merkin, S.K. Scott, Phys. Chem. Chem. Phys. 2 (2000) 4013.
- [19] J.R. Bamforth, J.H. Merkin, S.K. Scott, R. Tóth, V. Gáspár, Phys. Chem. Chem. Phys. 3 (2001) 1435.
- [20] J.R. Bamforth, R. Tóth, V. Gáspár, S.K. Scott, Phys. Chem. Chem. Phys. 4 (2002) 1299.
- [21] S.P. Kuznetsov, E. Mosekilde, G. Dewel, P. Borckmans, J. Chem. Phys. 106 (1997) 7609.
- [22] P. Andresen, M. Bache, E. Mosekilde, Phys. Rev. E 60 (1999) 297.
- [23] M. Kaern, M. Menzinger, Phys. Rev. E 60 (1999) 3471.
- [24] J.B. Keller, S.I. Rubinow, J. Chem. Phys. 74 (1981) 5000.
- [25] I. Lagzi, Phys. Chem. Chem. Phys. 4 (2002) 1268.
- [26] A. Büki, É. Kárpáti-Smidróczki, M. Zrinyi, Physica A 220 (1995) 357.